DEVELOPMENTAL DYNAMICS 238:3139–3151, 2009

RESEARCH ARTICLE

High Resolution Cell Lineage Tracing Reveals Developmental Variability in Leech

Stephanie E. Gline,* Dian-Han Kuo, Alberto Stolfi, and David A. Weisblat

Knowing the normal patterns of embryonic cell proliferation, migration, and differentiation is a cornerstone for understanding development. Yet for most species, the precision with which embryonic cell lineages can be determined is limited by technical considerations (the large numbers of cells, extended developmental times, opacity of the embryos), and these are exacerbated by the inherent variability of the lineages themselves. Here, we present an improved method of cell lineage tracing in the leech *Helobdella*, driving the expression of a nuclearly localized histone H2B:GFP (green fluorescent protein) fusion protein in selected lineages by microinjection of a plasmid vector. This construct generates a long lasting and minimally mosaic signal with single cell resolution, and does not disrupt the development of most lineages tested. We have validated this technique by elucidating details of cell lineages contributing to segmental and prostomial tissues that could not be observed with standard dextran lineage tracers. *Developmental Dynamics 238:3139–3151,* 2009. © **2009 Wiley-Liss, Inc.**

Key words: leech; Helobdella; plasmid injection; cell lineage variability

Accepted 5 October 2009

INTRODUCTION

Cell lineage-dependent patterning processes are broadly implicated in metazoan development. In the nematode *Caenorhabditis elegans*, for example, all 1,090 somatic cells in the adult hermaphrodite arise by essentially invariant lineages (Sulston et al., 1983). Skilled observers can complete precise lineage analyses for *C. elegans* by direct observation, thanks to the rapid development (less than 15 hr from zygote to hatching), small number of cells, and transparency of its embryos (Sulston et al., 1983).

In most animals, however, embryonic cell lineages can be observed and described with only limited precision and completeness.

In the leech *Helobdella* for example, embryogenesis takes approximately 10 days and its large yolky embryo poses significant challenges for visualization, compounded by the fact that *Helobdella* generates juveniles containing over 50,000 cells. Even such moderately complex embryos provide a technical challenge in analyzing cell lineages, and thus in establishing the extent to which cell lineages are determinate. To circumvent these problems, embryonic cell lineages in *Helobdella* and other systems have been studied using microinjected intracellular lineage tracers (Weisblat et al., 1978; Zhang and Weisblat, 2005). Here, we present a modified cell lineage tracing technique based on plasmid injection, which provides a significant improvement on previous methods in *Helobdella* and will hopefully be of use in other cellularly complex embryos.

As a glossiphoniid leech, *Helobdella* is a segmented representative of the superphylum Lophotrochozoa. Segmental mesoderm and ectoderm arise from a posterior growth zone (PGZ) comprising five bilateral pairs of lineage-restricted stem cells (M, N, O/P, O/P, and Q teloblasts), and the initial divisions of the teloblast progeny (the m, n, o, p, and q blast cell clones) are highly stereotyped (Fig. 1; Zackson, 1984; Shankland, 1987a,b; Bissen and

Additional Supporting Information may be found in the online version of this article.

Department of Molecular and Cell Biology, University of California, Berkeley, California

Grant sponsor: NIH; Grant number: R01 GM074619.

***Correspondence to: Stephanie E. Gline, Department of Molecular and Cell Biology, 385 Life Sciences Addition, University of California, Berkeley, CA 94720-3200. E-mail: sgline@berkeley.edu**

DOI 10.1002/dvdy.22158
Published online 16 November 2009 in Wiley InterScience (www.interscience.wiley.com).

Weisblat, 1989; Zhang and Weisblat, 2005). Intracellularly injected lineage tracers were first developed for use on *Helobdella* embryos, including horseradish peroxidase (HRP; Weisblat et al., 1978), fluorescently modified peptides (Weisblat et al., 1980) and the now standard fluorescent dextrans (Gimlich and Braun, 1985). More recently, nuclear localized fluorescent proteins (nXFPs) expressed from injected mRNAs have been used for cell lineage analysis in this system (Zhang and Weisblat, 2005). nXFPs are useful because they permit more precise determination of cell position and cell number than can be achieved with tracers distributed throughout the cytoplasm, especially as the cellular complexity of the embryo increases during development (Zhang and Weisblat, 2005). However, degradation of injected mRNAs leads to decreasing levels of even the relatively stable XFP proteins in older embryos (Zhang and Weisblat, 2005). Moreover, nXFPs disperse as the nuclear envelope breaks down during mitosis, impeding the analysis of complex lineages.

Plasmid DNA may be more stable than mRNA and can be continuously transcribed in those cells that inherit it. Plasmid injections into nuclei of postmitotic cells have been used in late stage embryos of the medicinal leech *Hirudo* to express reporter constructs as well as for functional studies (Baker and Macagno, 2006, 2007; Shefi et al., 2006; Baker et al., 2008). Previous attempts to drive ectopic gene expression in the early *Helobdella* embryo using plasmid injections were problematic, however; expression was highly mosaic (i.e., was seen in only a few of the progeny of the injected cell), and the injected lineage developed abnormally independent of the expression of the transgene.

In the experiments reported here, we have used an improved plasmid construct in which leech EF1alpha promoter (Pilon and Weisblat, 1997) drives the expression of a leech histone2B fused to green fluorescent protein (pEF-H2B:GFP). Injection of this construct resulted in long-lasting, robust expression of the transgene in the progeny of injected cells. Plasmid injection and expression of H2B:GFP transgene did not appear to disrupt normal development in most lineages, although some lineages were more sensitive to plasmid injections than others.

Using this construct in conjunction with a standard cytoplasmic lineage

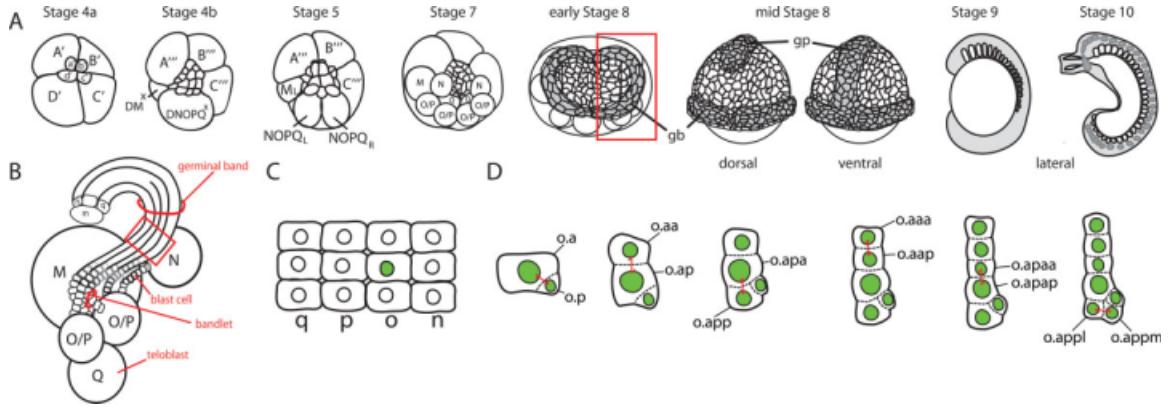

Fig. 1.

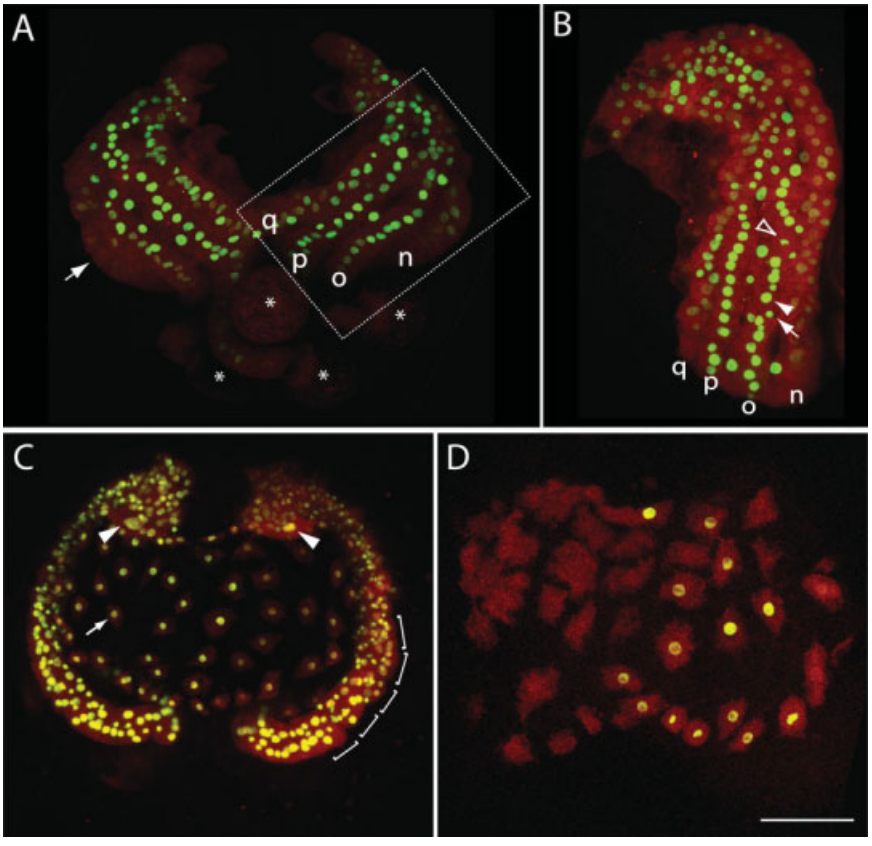

Fig. 2.

tracer rhodamine dextran (RDA), we were able to follow an o blast cell sublineage (o.app), which contributes a clone of purely epidermal progeny (Shankland, 1987a), from its birth through differentiation. While the first division in this sublineage is as stereotyped as those leading up to it, subsequent divisions are not, consistent with a transition from tightly regulated cell divisions in early development to a more stochastic process as cellular complexity increases.

RESULTS

Summary of Leech Development

Leech development proceeds by means of a modified version of spiral cleavage (Whitman, 1878; Bissen and Weisblat, 1989; Dohle, 1999) that generates 25 micromeres, 3 macromeres and 10 segmentation stem cells (teloblasts; Fig. 1A). Micromere lineages contribute progeny to prostomial tissue and to provisional and definitive epidermis (Weisblat et al., 1984; Nardelli-Haefliger and Shankland, 1993; Huang et al., 2002). Segmental ectoderm, and mesoderm are derived from the five bilateral pairs of teloblasts (Fig. 1A; Weisblat et al., 1980; Shankland and Savage, 1997); each teloblast lineage contributes a stereotyped, segmentally iterated complement of progeny. Teloblasts undergo iterated highly asymmetric divisions with cell cycle durations of approximately 75 min to produce columns of segmental founder cells (blast cells), which coalesce ipsilaterally to form germinal bands (Fig. 1B,C). The left and right germinal bands join at their anterior ends and move over the surface of the embryo, coalescing into a bilaterally symmetric germinal plate, from which the segmental tissues differentiate (Fig. 1A). In *Helobdella*, the early blastomeres are amenable to microinjection and with few exceptions, early development proceeds by means of determinate lineages (Bissen and Weisblat, 1989; Smith and Weisblat, 1994; Huang et al., 2002).

pEF-H2B:GFP Drives Transgene Expression in Proteloblast Lineages

Previous plasmid injections in *Helobdella* were found to disrupt development of the injected lineage (Pilon and Weisblat, 1997). Here, the DNA concentrations (96 ng/μl) used are 40-fold lower than in previous experiments (Pilon and Weisblat, 1997) and an intron between the promoter and reporter gene in the previous construct has been deleted (see the Experimental Procedures section). To test the effects of pEF-H2B:GFP on development, we first injected it into the ectodermal proteloblast (i.e., cell DNOPQ, DNOPQ′, DNOPQ″ or DNOPQ‴, designated collectively as DNOPQ^x, in embryos ranging from 12 to 20 hr after zygotic deposition (AZD) during stage 4; see Fig. 1A). These cells were chosen because deviations in their normal cleavage patterns would be obvious. Co-injecting RDA with the plasmid allowed us to assess the mosaicism of the plasmid-driven gene expression, by comparing the distributions of RDA- and GFP-labeled cells. Embryos at mid-stage 8 (78 to 120 hr after injection) were scored for normal development, as judged by the presence of the normal complement of eight ectoteloblasts, blast cell progeny arranged into left and right germinal bands and by the blast cell division patterns within individual lineages as revealed by the expression of the H2B:GFP transgene (Fig. 2A,B).

By these criteria, the success of the injections varied. Pooling the 7 most successful of 10 experimental clutches, 80% of the embryos (63/79 embryos) developed normally, while in the other three clutches, only 31% of the injected embryos (47/152 embryos) developed normally; typically, success rates of 90% or more are achieved when RDA alone is injected. Most of the RDA-

Fig. 1. Relevant aspects of leech development. **A**: Diagrammatic representations of selected stages (animal pole views unless otherwise indicated). In the eight-cell embryo (stage 4a), the D quadrant has cleaved to form micromere d′ and macromere D′, the teloblast precursor. At stage 5, macromere D′ has given rise to left and right mesodermal and ectodermal precursors (M teloblasts and NOPQ proteloblasts, respectively, the right M teloblast is out of view at the vegetal pole). At stage 7, all five pairs of teloblasts are present. At early stage 8, teloblasts have produced columns of segmental founder cells called germinal bands (gb, gray; see panel B for details); germinal bands and the territory between them are covered with a provisional epithelium generated by micromeres. At mid-stage 8, the lengthening germinal bands have begun to coalesce along the prospective ventral midline to form the germinal plate (gp), from which segmental mesoderm and ectoderm arise. During stages 9 and 10, segments differentiate and the germinal plate expands from ventral to dorsal territory, displacing the micromere-derived epithelium (not shown at these stages). **B**: Schematic of a stage 8 embryo, corresponding to the boxed section in panel (A), showing the relationships of teloblasts, blast cells, bandlets, and germinal band. Teloblasts mark the posterior growth zone and the older, more distal blast cells contribute to more anterior segments. **C**: Arrangement of undivided ectodermal blast cells within the germinal band, corresponding to the boxed section of panel (B); a single o blast cell is highlighted with a green nucleus. The mesodermal bandlet lies beneath the ectoderm and is not shown. **D**: Schematics showing the first six divisions of an o blast cell clone in the right germinal band; at each division the sister cells are named by adding a letter to indicate their relative positions at the end of cytokinesis, a, anterior; p, posterior; l, lateral; m, medial. In each panel, sister cells of the most recent division are indicated by red double arrows.

Fig. 2. Expression of H2B:GFP in the DNOPQ^x and DM^x lineages. In this and all figures, anterior is up, cytoplasmic RDA lineage tracer is red, nuclear H2B:GFP is green, and images are maximum projections of stacks of confocal images, unless otherwise noted. **A**: Animal pole view of an embryo whose DNOPQ^x had been injected with RDA and pEF-H2B:GFP 78 hr before fixation at early stage 8 (see Fig. 1A,B). This image shows blast cell bandlets in the left and right germinal bands (labeled in the right germinal band) and some teloblasts (asterisks); not all labeled cells are visible because the stack does not extend through the entire embryo. Note the reduced levels of transgene expression in the left n bandlet (arrow). **B**: Animal view of a sibling embryo fixed 96 hr after injection, showing the right germinal band, comparable to the region enclosed in the dotted box in A. Normal divisions of blast cells in the o bandlet are indicated by the presence of identifiable cells including o.p (white arrow), o.a (white arrowhead), and a mitotic o.a cell (open arrowhead). **C**: An embryo whose DM^x was injected with RDA and pEF-H2B:GFP 4 days before fixation at early stage 8. Within the germinal bands, proliferation of individual m blast cell clones produce developing hemi-somites (brackets). In the region between the germinal bands, migratory, nonsegmental freckle cells derived from the mesodermal lineage are evident (arrow) and additional nonsegmental cells with exceptionally broad nuclei (arrowheads) are seen at the anterior of the left and right germinal bands. **D**: Higher magnification image of freckle cells in a sibling embryo showing mosaic transgene expression. Scale bar = 100 μm in A,C, 50 μm in B, 75 μm in D.

labeled cells in the normally developing embryos exhibited robust GFP fluorescence in their nuclei, indicative of H2B:GFP expression and localization (Fig. 2A,B). The spatial distributions and size differences of GFP-labeled nuclei in the individual ectodermal bandlets also corresponded to previous descriptions of blast cell division patterns (Figs. 1D, 2B; Zackson, 1984; Shankland, 1987a,b; Bissen and Weisblat, 1989), indicating that the plasmid injection and consequent expression of the H2B:GFP transgene had not significantly perturbed development.

The success rate of the plasmid injections varied in a stage-dependent manner. For example, none of the experiments in which zygotes (stage 1) were injected yielded normal embryos (data not shown), whereas, the majority of embryos (66/78 or 85% overall in five experiments) developed normally for injections of the unilateral ectodermal precursors NOPQ^{x} (i.e., cell NOPQ, NOPQ′ or NOPQ″) at stage 5 (Fig. 1A; Supp. Fig. S1 and Supp. Table S1, which are available online).

Closer inspection of the plasmid-injected embryos revealed that the H2B:GFP signal was not uniform in all the RDA-labeled progeny of the injected blastomere (Fig. 2). Moreover, in some embryos, one or more of the RDA-labeled ectodermal lineages showed low or no transgene expression, indicative of mosaic expression of the injected plasmid (Fig. 2, Supp. Fig. S1, and data not shown). Curiously, the mosaicism of transgene expression was increased, rather than decreased when the plasmid was digested with I-*Sce*I meganuclease before injection (Supp. Fig. S1, and Supp. Table S1).

To compare the efficacy of transgene expression in segmental mesoderm with that observed in the ectodermal lineages, we injected the mesodermal precursor DM, DM′, or DM″ (collectively designated DM^{x}) with a mixture of RDA and pEF-H2B:GFP. As with DNOPQ^{x}, injecting plasmid into the DM^{x} proteloblasts disrupted development of the mesodermal lineage to a somewhat greater extent than did standard lineage tracers; 72% (33/46 embryos in three experiments) had developed normally when scored 4–5 days after injection. As with the NOPQ^{x} vs. DNOPQ^{x} comparisons, plasmid injection into individual M teloblasts was less disruptive of normal development than injection into DM^{x}; 88% of M-injected embryos (46/52 embryos in three experiments) developed normally.

Expression of the transgene was robust in the mesodermal lineage (Fig. 2C) and exhibited a range of mosaicism similar to experiments in which pEF-H2B:GFP was injected into the ectodermal proteloblasts. Expression of the transgene was most likely to be mosaic or absent in the cells arising early on in the M lineage, including a group of nonsegmental, mesenchymal "freckle cells," which lie between the germinal bands at early stage 8 and arise from cells born early on in the mesodermal lineage (Fig. 2C,D; Zackson, 1982; Nelson and Weisblat, 1991, 1992; Chi, 1996). The transgene lineage tracer revealed another set of M-derived nonsegmental cells that have not been previously described: large cells with flattened nuclei at the anterior lateral portion of the left and right mesodermal germinal bands (Fig. 2C; S.E.G., unpublished observations).

Transgene Expression and Perdurance in Teloblast Lineages

A major goal of this work was to develop a technique that would facilitate determination of the complete lineages of the identifiable neurons comprising the segmental nervous system of the leech (Muller et al., 1981). For this purpose, long-lasting nondisruptive expression of the fluorescent, nuclearly localized transgene product and compatibility with time-lapse imaging are key features.

Using plasmid-driven expression of H2B:GFP as the lineage tracer, we were able to make time-lapse videos of sufficiently high frame rate and long duration to capture sequential divisions of o blast cells (Fig. 3A, and Supp. Movie S2). With the H2B:GFP reporter, we could follow chromatin morphology throughout highly asymmetric divisions; intriguingly, asymmetries in chromatin volume between the cells o.a and o.p were evident before the nuclei had reformed (Fig. 3A, and Supp. Movie S2).

To test the perdurance of plasmid-driven H2B:GFP expression in teloblast lineages, we injected individual teloblasts with pEF-H2B:GFP and tested for normal development of the labeled lineages by comparing the patterns of labeled nuclei with expectations based on numerous previous studies. Here, we focused on the O lineage because the O-derived pattern elements have been described previously and are relatively easy to identify (Shankland and Weisblat, 1984; Weisblat and Blair, 1984; Zackson, 1984; Shankland, 1987a).

We injected individual O/P teloblasts in numerous embryos and fixed samples at times ranging from 3 to 10 days after injection. The majority of all batches injected exhibited normal development, as judged by the timing and orientation of inferred blast cell divisions at approximately 3 days after injection (Fig. 3B) and by the distribution of RDA- and GFP-labeled progeny at 6 to 10 days after injection (Fig. 3C–E).

The one exception to the essentially nonmosaic expression in these experiments was in embryos in which the first blast cell clone labeled with RDA showed very low levels of H2B:GFP expression, compared with the rest of the injected lineage (Fig. 3C). The occasional failure of transgene expression in the clone of the first blast cell produced after injection was consistent with the expected differences in diffusional mobility between the plasmid (2,000 kDa) and the RDA (10 kDa on average). Thus, when teloblasts were, by chance, injected late in the cell cycle, the cytokinetic furrow would have closed off the nascent blast cell before the larger molecule could diffuse from the site of injection into the nascent blast cell.

For embryos fixed at stage 8 and beyond, it is possible to dissect the germinal bands and/or germinal plate from the yolk, for analysis by confocal microscopy. In such preparations, pattern elements corresponding to previously described clusters of segmentally iterated cells could be identified. For example, in stages 9–11, the O lineage in each segment includes differentiated neurons in anterior dorsal (AD), crescent-shaped (CR), and posterior ventral (PV) clusters within the

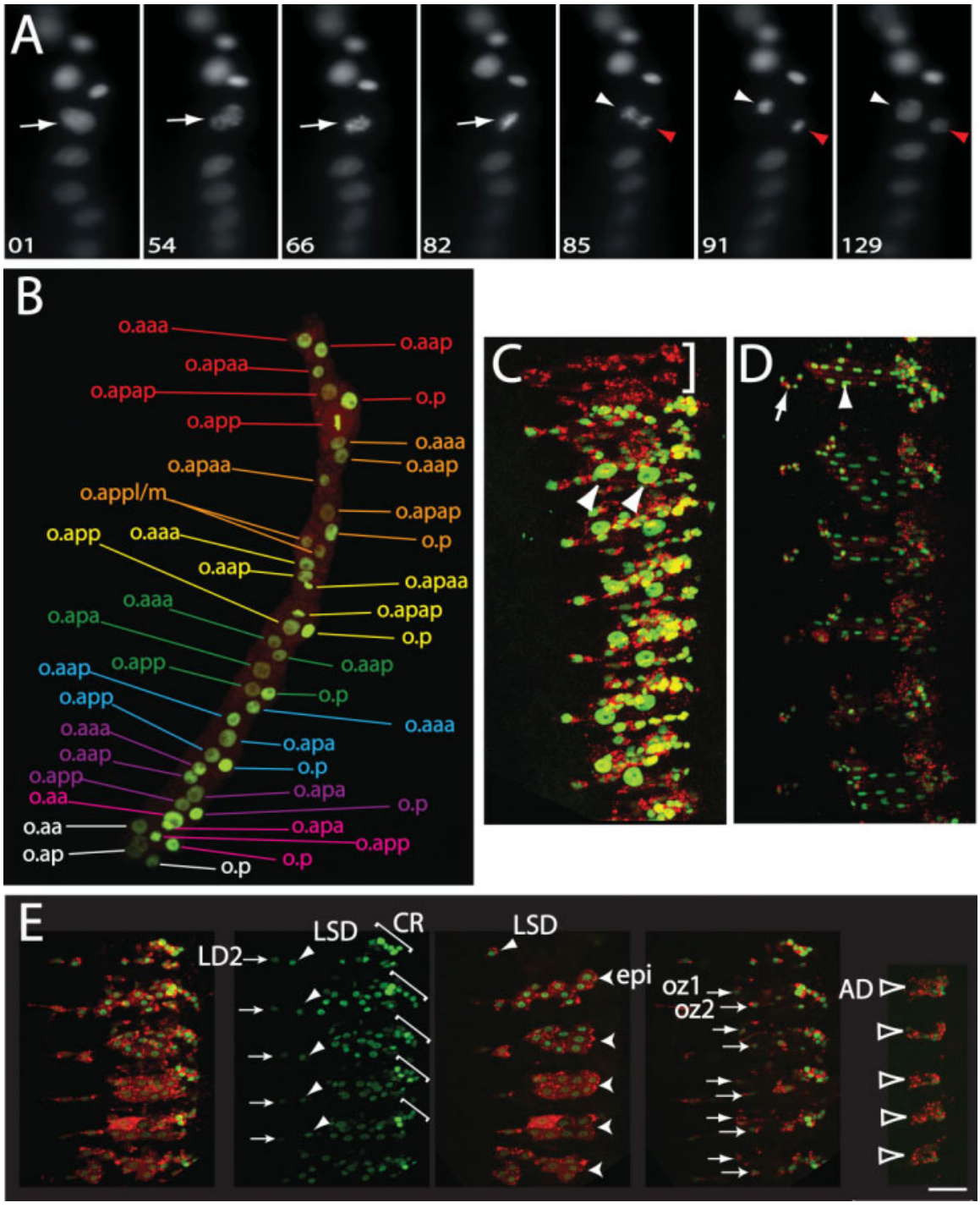

Fig. 3. Expression of pEF-H2B:GFP in the O lineage. **A**: Frames from a time-lapse video (one image per min, 199 min total duration) showing the division of a primary o blast cell (white arrow) to form sister cells o.a (white arrowhead) and o.p (red arrowhead). In this field of view, two pairs of o.a and o.p sister cells are visible (see Fig. 1C), slightly out of focus, anterior to the dividing cell, and undivided primary blast cells lie posterior to it. Elapsed time (minutes since the start of imaging) is indicated in bottom left hand corner. B–E: Maximal projections of confocal stacks of O lineages labeled with RDA and pEF-H2B:GFP in embryos fixed at various time points after injection. **B**: Seventy-two hours after injection; anterior portion of the o bandlet. Early progeny of the o clones are indicated, with distinct colors for each clone (cell nomenclature as in Fig. 1C). **C**: One hundred forty-four hours after injection; anterior portion of a dissected germinal plate. Bracket marks progeny of first labeled blast cell clone, which is not expressing the transgene. Differentiated epidermal cells can be distinguished by their broadened nuclei (arrowheads) and by their superficial location. **D**: Two hundred six hours after injection; anterior portion of the germinal plate. By this time, green fluorescent protein (GFP) transgene expression was no longer visible by direct fluorescence. This embryo was visualized by fluorescent immunostaining against GFP (green). Progeny of o.aa, (arrow) can be distinguished from o.app derived epithelial cells (arrowhead). **E:** Labeled O pattern elements. Views of six segments from the anterior portion of a germinal plate dissected from an embryo fixed 144 hr after injection. The two left-hand panels are maximal projections from the complete stack of confocal images; the second panel shows GFP signal only, to better visualize the nuclei corresponding to the secondary lateral dopaminergic cell (LD2), the o.aa-derived lateral skin dot (LSD) and the ganglionic crescent (CR). The three right-hand panels show partial stacks corresponding to superficial (ventral surface), medial, and deep optical sections, highlighting o.app-derived epidermal cells (epi), O-derived peripheral neurons (oz1 and oz2), and a group of anterodorsal ganglionic cells (AD), respectively. Note that, in the anteriormost segment, the o.app-derived epidermis, oz1, and AD neurons are not labeled, because they are contributed to by the next anterior, unlabeled o blast cell clone (Weisblat and Shankland, 1985). Scale bar = 10 μm in A,B; 33 μm in C; 37 μm in D; 35 μm in E.

segmental ganglion, plus three peripheral neurons (oz1, oz2, and LD2) and a lateral skin dot (LSD; Fig. 3E; Shankland, 1987a). As embryos reach the juvenile stage, H2B:GFP fluorescence declines and autofluorescence increases, perhaps in association with the emergence of differentiating pigment cells in the body wall. In these older animals, we were still able to generate a strong signal for the expressed transgene product by immunostaining for GFP (Fig. 3D).

Interspecies Difference and Intraspecies Variation in Blast Cell Division and Differentiation Patterns

The discrete nuclear localization of H2B:GFP fluorescence makes it possible to identify and count cells in individual pattern elements with a precision not previously available. Here, we have used this technique to determine the extent to which the stereotyped early blast cell division patterns persist later in development. Previous studies showed that cell o.app, a great-granddaughter of the o blast cell, gives rise to a clone comprising exclusively squamous epidermal cells in the posterior mediolateral portion of each segment in the congeneric species *H. triserialis* (see Fig. 1D for cell nomenclature; Shankland, 1987a). In contrast, cell o.aa contributes a clone of mixed cell types including a separate, smaller patch of epidermis that eventually merges with the larger o.app clone from the next anterior segment (Fig. 3B,E; Weisblat and Shankland, 1985; Shankland, 1987a); thus, in any given segment, these two patches of O-derived epidermis arise from two different blast cell clones. The further divisions within the o.app and o.aa clones have not been examined previously, because it was not possible to distinguish epidermal cell boundaries using cytoplasmic lineage tracers. Using H2B:GFP expression in conjunction with RDA as lineage tracers, we were able to identify and count the epidermal contributions from the O lineage in each segment at a variety of developmental times. For this purpose, the germinal plates were dissected from embryos fixed at various time points after injection and examined by confocal microscopy.

The mediolaterally oriented division of cell o.app to form cells o.appl and o.appm was first described in *Helobdella triserialis* (Shankland, 1987a), where it occurs at approximately 40 hr clonal age (cl.ag.), i.e., 40 hr after the birth of the o blast cell from which the o.app in question derives. We found that the homologous o.app cell in *Helobdella* sp. (Austin) undergoes an equivalent division, but significantly later than in *H. triserialis*. For example, in one experiment, only 5 of 13 embryos fixed 72 hr after injections contained segments in which o.app had divided. In one of these embryos, o.app had divided in the first five labeled segments, suggesting that the anteriormost labeled o.app had divided at approximately 66 hr cl.ag. in that embryo. Yet in sibling embryos, that division had not yet occurred at 72 hr cl.ag. At the next time point from this experiment, 87 hr after injection, all 12 embryos fixed contained multiple segments in which o.app had divided. Thus, we estimate that the time window during which the o.app division occurs can be more than 5 hr among embryos of a single clutch and that o.app divides no earlier than 66 hr cl.ag., roughly 30 hr later than in *H. triserialis*. This interspecies difference is consistent with previously observed retardation of approximately 24 hr for primary blast cell cycles in *H. robusta* and this sibling species relative to *H. triserialis* (Bissen and Weisblat, 1989; Zhang and Weisblat, 2005).

Notwithstanding the differences in cell division times between species, and to a lesser extent among embryos of a given species, divisions of primary blast cells and their early progeny in any given embryo correlate closely with the order in which the blast cells arise from the parent teloblast; occasional cases are observed in which blast cells divide out of birth order, that is, a more posterior cell divides before its anterior counterpart (Fig. 3B; Zackson, 1984). Consistent with these previous findings, in just one of the five embryos fixed 72 hr after injection, we observed an o.app that had divided slightly "out of order." That is, the o.app cell in one segment had already completed its division while o.app in the next anterior segment was still in metaphase (Fig. 3B). In contrast to the small range of variation in timing of divisions in the o blast cell clones up to that of o.app, however, we observed considerably larger variability in the subsequent patterns of cell division and differentiation within the o.app clones, even in individual embryos, as detailed below.

Cells o.appl/m have a relatively long cell cycle (>35 hr) during which they undergo morphological differentiation. Differentiation of the first O-derived epidermal cells was judged by their large nuclear profile and flattened morphology (Figs. 3C, 4). These two epidermal cells then further proliferate (Figs. 3D,E, 4) and the timing of their subsequent divisions is no longer tightly linked to birth order. By their positions and by comparison with previous studies, we interpreted these cells as morphologically differentiated o.appl and o.appm cells. Epidermal differentiation was observed as early as 88 hr cl.ag. in some segments (not shown), but there was considerable variability in the timing of the differentiation. For example, in one batch of embryos fixed 99 hr after injection, some embryos contained as few as three and others as many as nine segments with pairs of labeled, differentiated epithelial cells (Fig. 4B).

The rate of cell proliferation in the o.app clones was also variable. For example, in one embryo, only two morphologically differentiated epidermal cells could be seen in each of 15 segments (cl.ag.124–141.5 hr), and hence neither o.appl nor o.appm had divided; but in another embryo from a separate batch, three epidermal cells in an o.app clone were observed as early as 105.5 hr cl.ag. Even within individual embryos, the number of o.app descendents did not increase monotonically with o blast cell clonal age (Fig. 4B). While we observed a general trend of increasing cell number among the o.app progeny in older clones (Fig. 4), clonal age did not reliably predict the number of cells in the o.app clone and embryos were commonly seen with multiple segments containing greater epidermal cell counts than their anterior neighboring segment (Fig. 4). Thus, by this point in development of the o.app

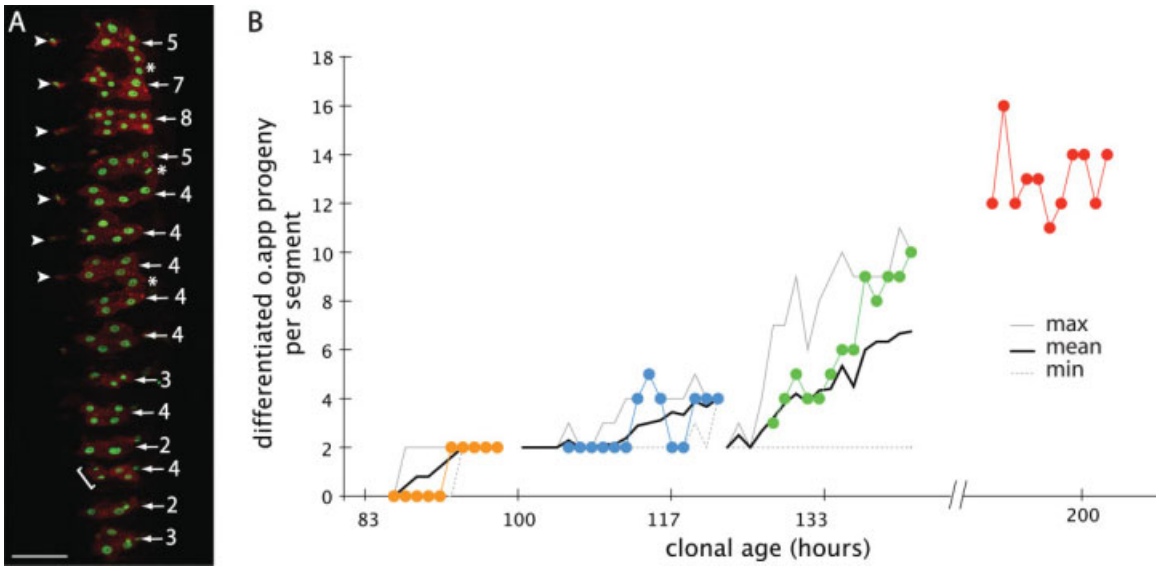

Fig. 4. Variability in the o.appl/m lineage. **A**: Partial confocal stack showing the ventral-most aspect of a dissected germinal plate, to highlight epidermal cells derived from o.aa (arrowheads) and o.aap (arrows) in an embryo fixed 144 hr after injection of the parent teloblast with rhodamine dextran (RDA) and pEF-H2B:GFP. In this partial stack, o.aa-derived epidermal cells are not visible in posterior segments due to the curvature of the embryo. Numbers refer to count of o.app progeny per segment. Asterisks indicate the merger of o.app-derived epidermal clusters between neighboring segments. Proliferation of morphologically differentiated epidermal cells is evidenced by cells dividing in the plane of the epithelium (bracket and middle asterisk). **B**: Graphical representation of segment-by-segment o.app-derived epidermal cell counts vs. clonal age in 21 embryos fixed at various time points. Gray and black lines indicate the maximum, minimum, and mean values obtained for each clonal age for which multiple specimens were examined. We did not interpolate between batches. Colored lines and dots represent data obtained from four individual specimens spanning various age ranges. Scale bar = 25 μm.

clones, the timing of cell divisions had become decoupled from the birth order of the parent blast cells.

In contrast to the o.app-derived epidermal clone, morphological differentiation of the laterally situated o.aa-derived epidermal cell (which generates the lateral skin dot; LSD) was first observed at clonal age 125 hr, and we never observed more than a single labeled o.aa-derived epidermal cell at clonal ages up to 144 hr (Fig. 3E). Even in the most advanced embryos examined, corresponding to cl.ag. 204 hr, a maximum of three o.aa-derived epidermal cells were observed in the first labeled segment, where the separate contributions of o.aa and o.app-derived epidermal cells could be unambiguously distinguished (Fig. 3D).

Long-Lasting Expression Reflects Ongoing Transcription From the Injected Plasmid

The perduring expression we observed from injecting pEF-H2B:GFP into precursors of diverse lineages in the *Helobdella* embryo might represent either transcription of the transgene throughout the injected lineage, and/or inheritance of protein and/or mRNA produced in an early burst within the injected cell and its immediate progeny. To distinguish the relative contributions of these possibilities, we injected plasmid encoding nGFP driven by the EF1-alpha promoter (pEF-nGFP) into the N teloblast lineage and then, after culturing the embryos for various periods of time, processed them by in situ hybridization for *gfp* transcripts. For comparison, we injected N teloblasts in sibling embryos with nGFP mRNA and processed them in parallel with plasmid-injected embryos (Zhang and Weisblat, 2005).

The results showed that transcription of the transgene occurred throughout the progeny of the injected cell. Transcript was readily detected in the plasmid-injected embryos by 21 hr after injection, but at this time transcript levels were clearly lower than in mRNA-injected embryos (Fig. 5A). Moreover, in contrast with the mRNA-injected embryos, transcript levels in plasmid-injected specimens were higher in the blast cells than in the injected teloblast itself, as judged by the intensity of the in situ staining (Fig. 5A). Consistent with previous results (Zhang and Weisblat, 2005), the decreased intensity of in situ staining was evident throughout the labeled lineage in mRNA-injected embryos as early as 71 hr after injection. In contrast, the in situ signal in plasmid-injected embryos increased until around 90 hr after injection. After this time, a decrease in staining intensity was first evident in anterior territory, spreading posterior at later times as in mRNA-injected embryos (Fig. 5A).

While *gfp* in situ staining was generally homogenous in intensity throughout the mRNA-injected lineage, clear variations in staining intensity were evident among cells in the plasmid-injected lineages. This reflects variation in transcript accumulation between cells, possibly due to differential inheritance or expression of the plasmid (Fig. 5B). Control experiments using sense probe for the in situs showed no staining (data not shown), which confirmed that the in situ protocol was not detecting plasmid DNA. Comparisons of GFP fluorescence in plasmid-injected versus mRNA-injected lineages further confirmed the differences seen at the

protein level. By 6 days after injection, expression was clearly stronger in the plasmid-injected lineages than those injected with mRNA, as judged by GFP fluorescence (Fig. 5C). Thus, while, mRNA injections are preferable for studies requiring gene expression within less than 2 days after injection, plasmid injections are apt to be preferable for studies involving lineage tracing or ectopic gene expression at later time points.

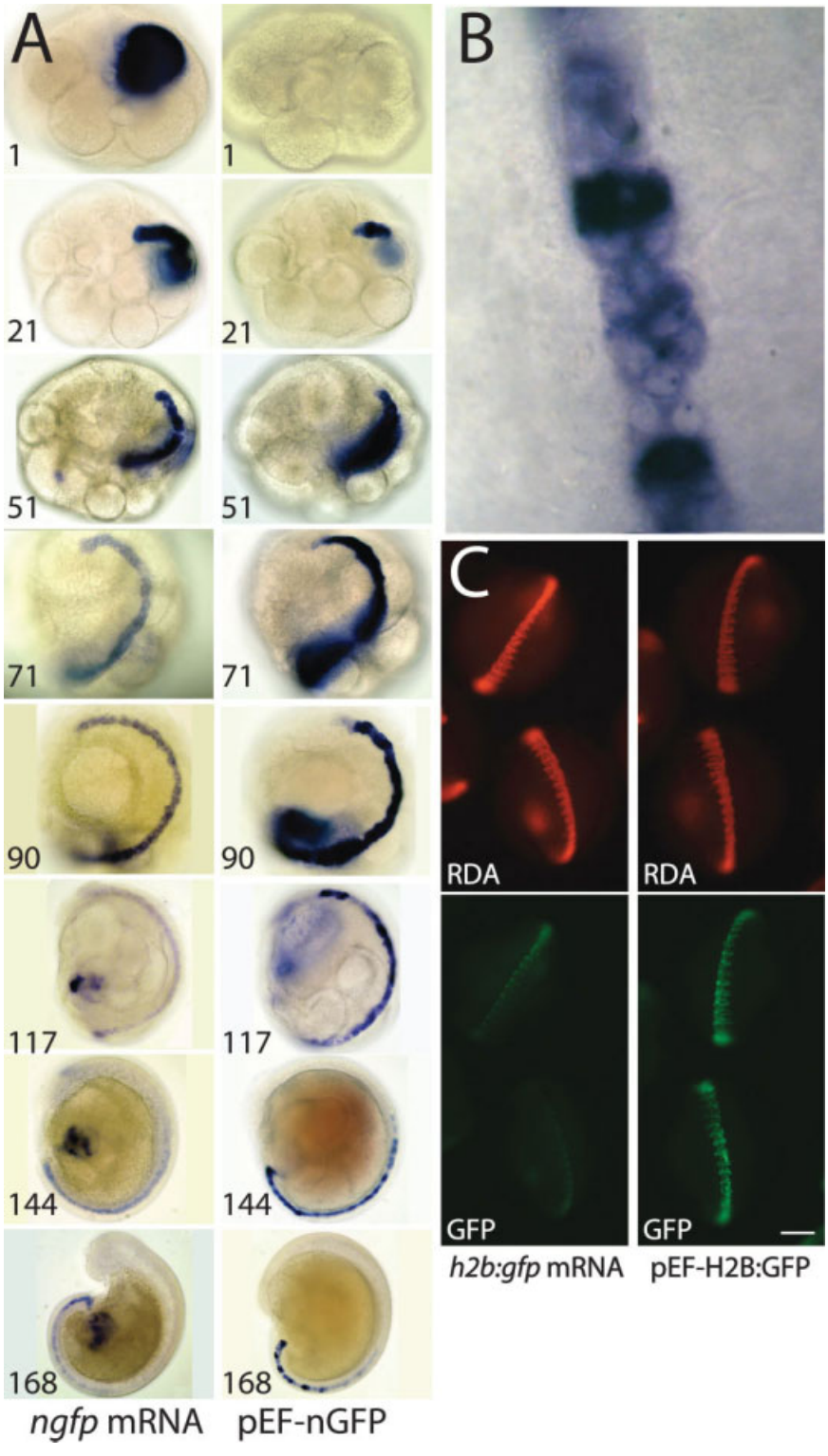

Fig. 5.

pEF-H2B:GFP Drives Transgene Expression in Micromere Lineages

To test expression of the transgene in nonteloblast lineages, we also injected pEF-H2B:GFP and RDA into the d′ micromere (Fig. 1A), 1 of 25 small cells arising during cleavage which contribute to various nonsegmental tissues of the embryo and adult (Smith and Weisblat, 1994; Huang et al., 2002). Cell cycle compositions and cell division patterns in the early micromere lineages have been described (Smith and Weisblat, 1994; Huang et al., 2002). Previous studies have shown that its early divisions in the d′ lineage are unequal and stem cell-like (Huang et al., 2002). The d′ lineage contributes progeny to the supraesophageal ganglion, definitive prostomial epidermis, proboscis muscle fibers and sheath, and to the epithelium of the provisional integument (Weisblat et al., 1984; Huang et al., 2002).

We injected the d′ micromere with pEF-H2B:GFP and RDA soon after its birth (7.5 hr AZD) and fixed embryos at various time points after injection. At 48 hr after injection, the stem cell-like divisions of the labeled micromeres were evidenced by a column of smaller cells extending vegetally from a larger cell, comparable to our previous findings using RDA lineage tracers alone (Fig. 6A; Huang et al.,

Fig. 5. Comparison of transcript distributions resulting from plasmid and mRNA injections. Right N teloblasts of stage 6a embryos were injected with rhodamine dextran (RDA) and either mRNA or plasmid encoding the same transcript, and examined at various time points after injection (1–168 hr). **A**: Brightfield images of embryos injected with *ngfp* mRNA or pEF-nGFP plasmid, fixed at the times indicated (hr after injection), and processed for green fluorescent protein (GFP) in situ hybridization; animal pole views are shown for embryos fixed 1–51 hr after injection and lateral views for embryos fixed 71–168 hr after injection. **B**: High power image of a portion of a bandlet in the posterior germinal plate of an embryo processed for nGFP in situ 96 hr after plasmid injection shows nonuniform distribution of transcript. **C**: Epifluorescent images of embryos injected with RDA and either *h2b:gfp* mRNA or pEF-H2B:GFP plasmid, and fixed 144 hr after injection. RDA signals are comparable, but the GFP signal has largely disappeared from the mRNA-injected embryos. Scale bar = 100 μm in A,C; 8 μm in B.

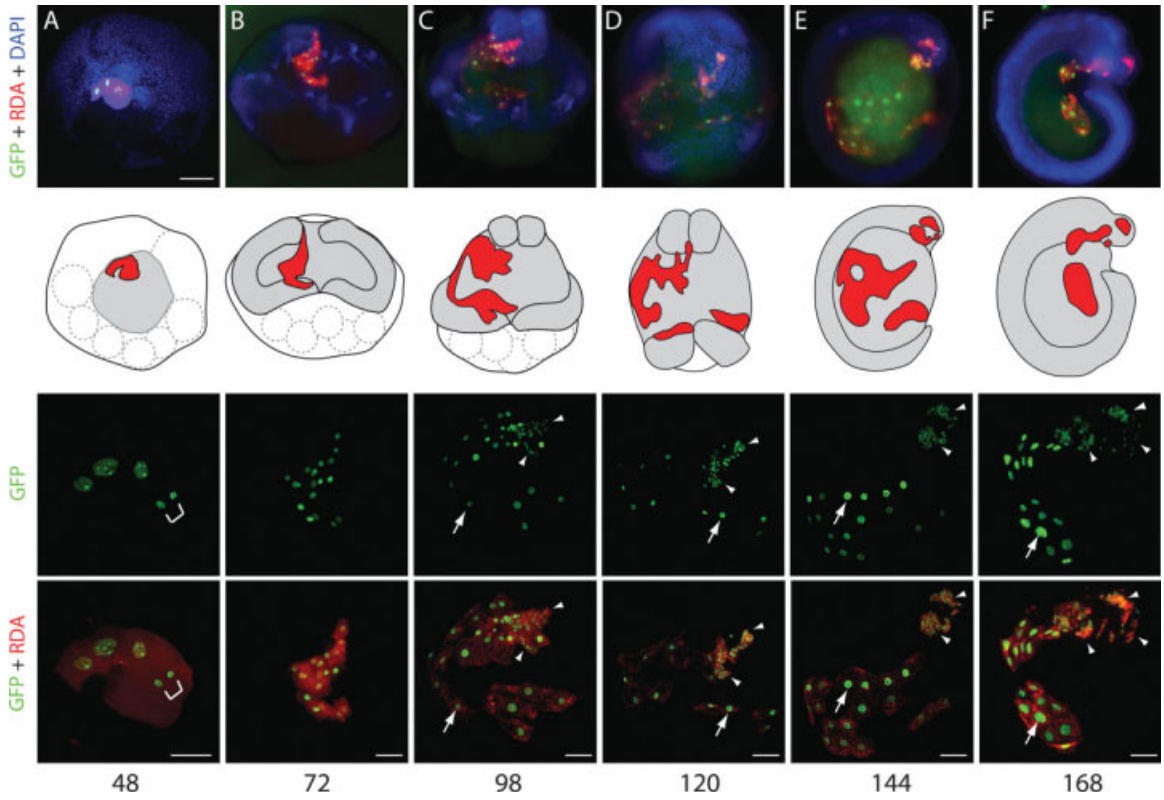

Fig. 6. Plasmid-driven transgene expression in a micromere lineage. Images of embryos in which micromere d′ was injected at approximately 15 min after its birth with RDA and pEF-H2B:GFP; injected embryos were fixed at a range of time points after injection (48–168 hr, as indicated below each panel). In each panel, the topmost images are a low power epifluorescence image of the entire embryo (RDA, red; H2B:GFP, green; DAPI [4′,6-diamidine-2-phenylidole-dihydrochloride] counterstain, blue, except that in panel (A), the blue color is autofluorescence) and a cartoon representation of that image to show the location of the labeled d′ clone. The two lower images in each panel are maximum projection confocal stacks as in other figures. **A**: The d′ lineage undergoes early stem-cell like divisions, and in this embryo the parental "stem cell" was captured completing mitosis (white bracket). **B–F**: At later time points, the d′ comes to comprise a mixed population of cells including provisional epithelial cells (arrows) and prostomial cells (arrowheads) that are readily distinguished based on differences in location, nuclear size, and cell morphology. Scale bar = 100 μm in upper panels; 20 μm in lower panels.

2002); by 72 hr, the d′ clones comprised roughly 20 contiguous cells (Fig. 6B).

By 98 hr after injection, two distinct populations of cells were evident within the d′ clone. One population, previously identified as epithelial cells of the provisional integument, comprised approximately two dozen superficial cells with large, flattened nuclei, left of the midline, outside the expanding margins of the germinal plate in dorsal territory (Fig. 6C; Weisblat et al., 1984). The other population comprised approximately 30 densely packed, deeper cells with small, spherical nuclei, left of the midline and anterior to the germinal plate, partially covered by the d′-derived epithelial cells (Fig. 6C); we interpreted these cells as precursors of definitive prostomial tissues (Weisblat et al., 1984; Nardelli-Haefliger and Shankland, 1993; Huang et al., 2002). Within this anterior population were two seemingly distinct subpopulations of smaller cells as judged by cell morphology and nuclear arrangement (Fig. 6C).

By 120 hr after injection, differences in nuclear diameters and cell density between the prostomial contributors and the larger epithelial cells were more apparent, and the epithelial cells no longer overlay the deeper cells at the anterior. The prostomial cells were more closely packed, and clearly separated into two distinct populations, while the epithelial cells had undergone few cell divisions and were continuing to spread into dorsal territory (Fig. 6D). By 144 hr after injection, the two anterior populations of prostomial cells had become physically separate (Fig. 6E), and the epithelial cells were further away from both populations of anterior cells (Fig. 6E). At 168 hr after injection, the anterior prostomial populations had further subdivided into several discreet populations of cells. The provisional epithelial cells were constricted toward the dorsal midline, ceding territory to the expanding germinal plate (Fig. 6F).

DISCUSSION

In the work presented here, we have explored the uses of plasmid-driven gene expression as a technique for tracing embryonic cell lineages in the leech *Helobdella*. Microinjecting circular plasmid, in which expression of a histone2B:GFP fusion protein is driven by a putative EF1-alpha enhancer, yielded robust expression of the transgene with unexpectedly low mosaicism, and with no obvious disruption of normal development in most experiments. Transgene transcript

was detected throughout the labeled lineages for up to 5 days after injection and protein was readily detected immunohistochemically at 10 days after injection. Variation in transcript levels detected between blast cell progeny suggests differences in rates of transgene transcription. Additionally, transcription is not limited to the parent teloblast, in which case we would expect to see uniform staining in all blast cells and darker staining in the teloblasts as in mRNA injections. Surprisingly, injecting the plasmid as the I-*Sce*I meganuclease restriction digest (Supp. Fig. S1, and Supp. Table S1) resulted in a dramatically reduced proportion of cells in the descendant clone expressing the transgene, which is contrary to results reported from other systems. No stable expression of the transgene was observed in any of the animals recovered in these experiments.

Of interest, we saw a cell type-dependent sensitivity to plasmid injections. Injections into zygotes never yielded normally developing embryos, and injections into the proteloblasts DM^x and $DNOPQ^x$ resulted in higher percentages of abnormal development of the injected lineage than injections into d′, the proteloblast $NOPQ^x$ or individual meso- and ecto-teloblasts. Expression of transgene after injecting the large yolky proteloblasts (DM^x, $DNOPQ^x$, and $NOPQ^x$) was typically more mosaic than after injecting individual teloblasts, and micromeres. This is most likely because the large sizes and the short cell cycles of these blastomeres make it more difficult for the slowly diffusing plasmid to distribute evenly in the cell before the first division after injection.

Comparisons With Other Microinjection-based Lineage Tracing Methods

Conventional lineage tracers such as RDA or other derivatized dextrans are distributed throughout the cytoplasm, which makes it difficult to resolve boundaries between adjacent labeled cells, especially when the progeny of the injected cell are small, densely packed and contain very little cytoplasm.

In contrast, the plasmid and mRNA injection techniques offer the advantage of expressing markers targeted to a specific subcellular organelle, which facilitates enumerating individual cells even within clusters of labeled cells. In the examples presented here, nuclear localization of the H2B:GFP made it possible to count individual cells within O-derived clusters of epidermal progeny, identify unique cells at the anterior end of the mesodermal germinal bands and allowed us to determine that the anterior portion of the d′ micromere lineage comprised many small cells instead of a few large ones.

Compared with the direct injection of mRNAs, the plasmid-injection method provides for longer lasting and temporally more uniform transcript levels. Injected mRNA is being degraded continuously from the time of injection, and compensating for this by injecting more mRNA disrupts normal development (Fig. 5; Zhang and Weisblat, 2005). In contrast, mRNA levels build up and decline more gradually after plasmid injection, which is useful for long-term experiments.

Disadvantages of the plasmid injection method include the delayed onset of expression compared with previous methods and varying degrees of mosaicism. The earliest detection of the expressed marker was between 14 and 48 hr after injection depending on the lineage injected, and at these early times, the level of expression was often lower than that obtained with mRNA injections. Mosaicism of transgene expression was observed when plasmid was injected into early blastomeres. However, this is not a major problem for cell lineage analysis in the leech, because progeny of these cells, such as micromeres and teloblasts, are amenable for microinjection and mosaicism is minimal when individual micromeres or teloblasts are injected.

Another consideration concerning the use of the plasmid-driven lineage tracing is the possibility of developmental disruptions. The risk of disrupting development is inherent in any experiment involving microinjection, but is compounded to the extent that the cells' metabolism is taken over to express exogenous genes. Our results suggest that for *Helobdella*, the large yolky blastomeres are particularly susceptible to developmental disruptions at the earliest stages of zygotic development and become progressively more resistant to such disruptions at later stages with the exception of the small and yolk-deficient first quartet micromeres.

Origins of Cell Lineage Variability

Previous studies in *Helobdella* and related species (Zackson, 1982, 1984; Bissen and Weisblat, 1989), building on the pioneering studies of annelid development carried out by E.B. Wilson (1892) and C.O. Whitman (1878), have illustrated that the early leech embryo exhibits stereotyped patterns of cell divisions comparable to those described for the nematode *Caenorhabditis elegans* (Sulston et al., 1983). Subsequent studies of leech development have focused largely on the segmental ganglia of the ventral nerve cord; in the first approximation, each adult ganglion contains approximately 200 pairs of individually identifiable neurons (Macagno, 1980), each of which is believed to arise by an invariant pattern of cell divisions from one of the five teloblast lineages during embryogenesis (Kramer and Weisblat, 1985; Weisblat and Shankland, 1985).

However, while the *C. elegans* larva hatches with precisely 558 cells, *Helobdella* contains roughly 50,000 cells as a juvenile; moreover, many nonneuronal cell types (e.g., muscles, epidermis, mesenchyme) continue proliferating postembryonically, so that the adult probably comprises several hundred thousand cells. It is implausible that such large numbers of apparently interchangeable cells would arise by fixed lineages, especially in light of the developmental plasticity inherent in the capacities for indeterminate growth, regeneration, and vegetative reproduction that are present in most annelid taxa. Even in *C. elegans*, significant variation is seen in cell cycle durations and in the positions of "identical" cells among embryos (Schnabel et al., 1997).

Thus, cell lineage variability in the *Helobdella* embryo is to be expected. Desjeux and Price (1999) documented

variability in the production of supernumerary blast cells from teloblasts, and we have previously documented variability in cell cycle composition for specific micromere lineages (Huang et al., 2002). Here, we used expression from injected plasmid to study variability in the o.app lineage, which gives rise only to epithelial cells (Shankland, 1987a). We find that the stereotypy of the o.app lineage breaks down some time after its division into o.appl and o.appm. Cells o.appl and o.appm both exhibit prolonged cell cycles; however, the subsequent divisions in the o.app clone are variable in timing, resulting in variation in the number of o.app-derived epithelial cells among different segments of the same individual at the juvenile stage. We have not excluded the possibility that the variability observed here in the o.app lineage reflects a cell-specific disruption of an otherwise stereotyped lineage by expression of the transgene or even the RDA itself. But given the normal development of the other O-derived sublineages in these same experiments, this possibility seems unlikely. Instead, we speculate that the o.aa lineage exhibits less variability than o.app due to constraints associated with the more tightly regulated production of specific neural cell phenotypes.

In conclusion, this study demonstrates the practicality of using plasmid injections to introduce persistent transgene expression in embryos of the leech *Helobdella*. Although we have exclusively focused on its use in cell lineage analysis here, this plasmid-based transgene expression method can be further adopted for gene *cis*-regulation analysis and for driving ectopic gene expression in functional analysis of developmental genes.

EXPERIMENTAL PROCEDURES

Embryos

Embryos of *Helobdella* sp. (Austin) collected from Austin, Texas, were obtained from a laboratory breeding colony. Embryos were cultured in HL saline and maintained at 23°C as described in Song et al. (2002). Staging and cell nomenclature are as defined previously (Weisblat and Huang, 2001) for *H. robusta*, but there are species differences in the cell cycle rates (Zhang and Weisblat, 2005; Gonsalves and Weisblat, 2007).

Isolation of a *Helobdella* Histone 2B Homolog

A 228 base-pair DNA fragment encoding a portion of histone 2B was amplified by polymerase chain reaction (PCR) from a commercially prepared, nondirectional cDNA library representing stage 7–10 embryos of *H. robusta* (Stratagene, La Jolla, CA), using degenerate primers (fwd = 5′-CARGTICAYCCIGAYCANGG-3′; rev = 5′-GTRTAYTTIGTIACNGCYTT-3′). This cDNA fragment was cloned into the pGEM-T Easy vector (Promega, Madison, WI) and sequenced. Additional coding sequence of *Hro-h2b* was amplified from the cDNA library using either a 3′ or 5′ extension primer (3′ extension = 5′-GGCTTCTC GCCTCGCCCACTACAACA-3′; 5′ extension = 5′-GTTGGCCAACTCGCCG GGTAACAGAA-3′) paired with a vector-specific primer (5′-CACTATAG GGCGAATTGGGTACC-3′). Amplicons from these PCR reactions were isolated, cloned into pGEM-T Easy and sequenced. The *Hro-h2b* cDNA sequence was then assembled from the sequences of individually cloned amplicons (Genbank accession #GQ280381) and the *Hro-h2b* DNA fragment to be introduced into pCS107 (gift from Richard Harland) was amplified from the cDNA library (fwd = 5′-TGGATCCAATGCCACCAAAGCCTGCC AGCAAGGGA-3′; rev = 5′-GGGTCGAC CTTTGAGCTGGTGTACTTGGTGACG GC-3′. A *Bam*HI restriction site was introduced at the 5′ end of the start codon and the 3′ stop codon was replaced with a *Sal*I restriction site.

Construction of pCS107-H2B-eGFP

pCS107-H2B-eGFP was used as the template for in vitro synthesis of mRNA. To construct pCS107-H2B-eGFP, a DNA fragment containing enhanced GFP (eGFP) coding region was first PCR-amplified from pCS2P-eGFP-X/P (Zhang and Weisblat, 2005) using the following primer pair: fwd = 5′-AGCGGCCGCTAGAAGGTGGC GGAATGG-3′; rev = 5′-CTCGAGTT ACTTGTACAGCTCGTCCAT-3′. The resulting DNA fragment contains the coding sequence of eGFP flanked by a *Not*I site and *Xho*I site at the 5′ and 3′ ends, respectively. The *egfp* DNA was introduced between the *Not*I and *Xho*I sites in the polylinker region of pCS107. *Hro-h2b* DNA was then introduced between the *Bam*HI and *Sal*I sites in the pCS107 polylinker.

Plasmid Constructs

A ~2.3-kb genomic DNA fragment that lies immediately upstream to the EF1alpha coding region was excised from pEF1NASS (Pilon and Weisblat, 1997) using *Eco*R1 and *Xba*1, and then purified by electrophoresis and gel extraction. pBSMN, a modified version of pBluescript, with I-*Sce*I sites flanking its multi-cloning sites (Ogino et al., 2006), was digested using *Eco*R1 and *Xba*1, treated with phosphatase and then purified by electrophoresis and gel extraction. The EF1alpha promoter fragment was then inserted into the digested pBSMN to create pBSMNEF1P.

pBSMNEF1P was first linearized with the restriction enzyme *Sal*I. The ends of linearized pBSMNEF1P were then blunted by Klenow fragment treatment. The blunted linear pBSMNEF1P was next digested with the restriction enzyme *Apa*I, yielding 20-bp and 5.3-kb fragments. The 5.3-kb fragment was treated with phosphatase and purified by electrophoresis and gel extraction.

To prepare the insert, the forward primer originally designed for cloning the coding region fragment of *Hro-h2b1* (5′-TGGATCCAATGCCACCAAA GCCTGCCAGCAAGGGA-3′) was paired with T3 primer (5′-ATTAACCCTCAC TAAAGGGAA-3′) to amplify the DNA fragment containing the coding region of H2B:eGFP and SV40 polyadenylation sequence. The PCR reaction was carried out using *Pfu* DNA polymerase (Stratagene), which generates blunt-end PCR products. The PCR product was then digested with *Apa*I. The *Apa*I digestion yielded 40-bp and 1.4-kb fragments. The 1.4-kb DNA fragment, containing the H2B:eGFP construct and the SV40 polyadenylation sequence was treated with polynucleotide kinase and purified by electrophoresis and gel extraction. The H2B-eGFP-SV40 DNA fragment was

then inserted into the processed pBSMNEF1P to create pEF-H2B:GFP.

pEF-nGFP was built using the same strategy for constructing pEF-H2B:GFP. The nls:eGFP-SV40 fragment was PCR-amplified from pCS2P-nls-eGFP (Zhang and Weisblat, 2005) using *Pfu* DNA polymerase. Forward primer corresponding to the area around the start codon of nls-eGFP (5′-AATGGCTCCAAAGAA GAAGCGT) and T3 primer were used in the PCR reaction. The PCR product was then digested with *Apa*I, treated with kinase, purified, and inserted into the processed pBSMNEF1P. Hence, the cloning strategy described here appears to be a convenient and widely applicable way for transferring pCS-based molecular constructs into pBSMNEF1P backbone.

Plasmid Purification, Plasmid Injection, mRNA Synthesis, and mRNA Injection

nGFP mRNA and h2bGFP mRNA were both transcribed in vitro from PCR amplicons generated from pCS2p-nls-eGFP (Zhang and Weisblat, 2005) and pCS107-H2B-eGFP plasmids, respectively, using SP6 and T3 primers. For this application, proofreading *Pfu* DNA polymerase was used for the PCR reaction. mRNA was transcribed from the amplicons using mMESSAGE mMACHINE SP6 kit (Ambion, Austin, TX). The concentration of mRNAs in the needle was 0.5 mg/ml with 8 mg/ml tetramethylrhodamine dextran (RDA; Molecular Probes, Eugene, OR). The final concentration of the plasmid in the injection needle was 96 mg/ml with 3 mg/ml RDA. Plasmids were purified using Qiagen MIDI Prep kits (Qiagen, Germantown, MD). Both mRNA and plasmid were co-injected with RDA lineage tracer.

Co-injection of Plasmid With I-*Sce*I

A total of 116 ng/μl of plasmid was preincubated with 0.5 units/μl of I-*Sce*I in 1X buffer (New England Biolabs, Ipswich, MA) at 37°C for 40 min in a volume of 5 μl. After incubation, 1 μl of 18 mg/ml RDA solution was added to the digest and the resultant mixture (with a final plasmid concentration of 96 ng/μl) was loaded into glass micropipets for injection.

Microscopy

For time-lapse fluorescence microscopy injected embryos were allowed to develop to desired stages, mounted in HL saline, then examined and photographed using a Nikon E800 epifluorescence microscope equipped with a cooled CCD camera (Princeton Instruments, Trenton, NJ), controlled by MetaMorph software (Molecular Devices, Sunnyvale, CA). For confocal microscopy, embryos were fixed for 1 hr at room temperature or o/n at 4°C in 0.75× phosphate buffered saline (PBS) in 4% paraformaldehyde. Images were acquired on a Leica SMRE microscope equipped with a TCS SL scanning head. Stacks of confocal images were processed using Image J (NIH) for color merging, 3D- and Z-projections.

In Situ Hybridization and Immunostaining

Antisense GFP probe was synthesized from linearized pCS2p-nls-eGFP using MEGAscript T7 kit (Ambion) and hybridization as previously described (Song et al., 2002). H2B:GFP localization in late stage 11 embryos and young juveniles was visualized by immunostaining of GFP. In short, specimens were first relaxed with relaxation buffer (4.8 mM NaCl, 1.2 mM KCl, 10 mM $MgCl_2$ and 8% EtOH) at 4°C, fixed with 4% formaldehyde in 0.5× phosphate buffered saline at 4°C overnight, washed with 1% Tween-20 in PBS (PBT) several times, and then blocked with 5% normal goat serum and 2% bovine serum albumin in PBT at room temperature for 2 hr. A rabbit anti-GFP polyclonal antibody (Invitrogen, Carlsbad, CA) was added at a 1:1,000 dilution in the blocking solution, and incubated at 4°C overnight. After several washes with PBT at room temperature, the specimens were placed in blocking solution, and Alexa Fluor 488 conjugated goat anti-rabbit secondary antibody (Invitrogen) was added at 1:600. The specimens were incubated at 4°C overnight, washed in PBT at room temperature for at least 6 hr with frequent buffer changes.

ACKNOWLEDGMENTS

We thank our colleagues for helpful discussions and the Levine lab for use of their confocal microscope. D.A.W. was funded by the NIH and A.S. was supported by an ARCS Fellowship.

REFERENCES

Baker MW, Macagno ER. 2006. Characterizations of Hirudo medicinalis DNA promoters for targeted gene expression. J Neurosci Methods 156:145–153.

Baker MW, Macagno ER. 2007. In vivo imaging of growth cone and filopodial dynamics: evidence for contact-mediated retraction of filopodia leading to the tiling of sibling processes. J Comp Neurol 500:850–862.

Baker MW, Peterson SM, Macagno ER. 2008. The receptor phosphatase Hm LAR2 collaborates with focal adhesion proteins in filopodial tips to control growth cone morphology. Dev Biol 320:215–225.

Bissen ST, Weisblat DA. 1989. The durations and compositions of cell cycles in embryos of the leech, Helobdella triserialis. Development 106:105–118.

Chi C. 1996. Freckle cells, an unique population of non-segmental mesoderm found during early leech development. Berkeley, CA: Thesis, Department of Molecular and Cellular Biology, University of Caifornia, Berkeley. 20 p.

Desjeux I, Price DJ. 1999. The production and elimination of supernumerary blast cells in the leech embryo. Dev Genes Evol 209:284–293.

Dohle W. 1999. The ancestral cleavage pattern of the clitellates and its phylogenetic deviations. Hydrobiologia 402: 267–283.

Gimlich RL, Braun J. 1985. Improved fluorescent compounds for tracing cell lineage. Dev Biol 109:509–514.

Gonsalves FC, Weisblat DA. 2007. MAPK regulation of maternal and zygotic Notch transcript stability in early development. Proc Natl Acad Sci USA 104:531–536.

Huang FZ, Kang D, Ramirez-Weber F-A, Bissen ST, Weisblat DA. 2002. Micromere lineage in the glossiphoniid leech Helobdella. Development 129: 719–732.

Kramer AP, Weisblat DA. 1985. Developmental neural kinship groups in the leech. J Neurosci 5:388–407.

Macagno ER. 1980. Number and distribution of neurons in leech segmental ganglia. J Comp Neurol 190:283–302.

Muller K, Nicholls J, Stent G. 1981. Neurobiology of the leech. Cold Spring Harbor, New York: Cold Spring Harbor Laboratory Press. 320 p.

Nardelli-Haefliger D, Shankland M. 1993. Lox10, a member of the NK-2 homeobox gene class, is expressed in a segmental pattern in the endoderm and in the cephalic nervous system of the leech Helobdella. Development 118:877–892.

Nelson BH, Weisblat DA. 1991. Conversion of ectoderm to mesoderm by cytoplasmic extrusion in leech embryos. Science 253:435–438.

Nelson BH, Weisblat DA. 1992. Cytoplasmic and cortical determinants interact to specify ectoderm and mesoderm in the leech embryo. Development 115: 103–115.

Ogino H, McConnell WB, Grainger RM. 2006. High-throughput transgenesis in Xenopus using I-SceI meganuclease. Nat Protoc 1:1703–1710.

Pilon M, Weisblat DA. 1997. A nanos homolog in leech. Development 124: 1771–1780.

Schnabel R, Hutter H, Moerman D, Schnabel H. 1997. Assessing normal embryogenesis in Caenorhabditis elegans using a 4D microscope: variability of development and regional specification. Dev Biol 184:234–265.

Shankland M. 1987a. Differentiation of the O and P cell lines in the embryo of the leech. I. Sequential commitment of blast cell sublineages. Dev Biol 123: 85–96.

Shankland M. 1987b. Differentiation of the O and P cell lines in the embryo of the leech. II. Genealogical relationship of descendant pattern elements in alternative developmental pathways. Dev Biol 123:97–107.

Shankland M, Savage RM. 1997. Annelids, the segmented worms. In: Gilbert SF, Raunio AM, editors. Embryology: constructing the organism. Sunderland, MA: Sinauer. p 219–235.

Shankland M, Weisblat DA. 1984. Stepwise commitment of blast cell fates during the positional specification of the O and P cell lines in the leech embryo. Dev Biol 106:326–342.

Shefi O, Simonnet C, Baker MW, Glass JR, Macagno ER, Groisman A. 2006. Microtargeted gene silencing and ectopic expression in live embryos using biolistic delivery with a pneumatic capillary gun. J Neurosci 26:6119–6123.

Smith CM, Weisblat DA. 1994. Micromere fate maps in leech embryos: lineage-specific differences in rates of cell proliferation. Development 120:3427–3438.

Song MH, Huang FZ, Chang GY, Weisblat DA. 2002. Expression and function of an even-skipped homolog in the leech Helobdella robusta. Development 129: 3681–3692.

Sulston JE, Schierenberg E, White JG, Thomson JN. 1983. The embryonic cell lineage of the nematode Caenorhabditis elegans. Dev Biol 100:64–119.

Weisblat DA, Blair SS. 1984. Developmental interderterminacy in embryos of the leech Helobdella triserialis. Dev Biol 101:326–335.

Weisblat DA, Huang FZ. 2001. An overview of glossiphoniid leech development. Can J Zool 79:218–232.

Weisblat DA, Shankland M. 1985. Cell lineage and segmentation in the leech. Philos Trans R Soc Lond B 312:39–56.

Weisblat DA, Sawyer RT, Stent GS. 1978. Cell lineage analysis by intracellular injection of a tracer enzyme. Science 202:1295–1298.

Weisblat DA, Harper G, Stent GS, Sawyer RT. 1980. Embryonic cell lineages in the nervous system of the glossiphoniid leech Helobdella triserialis. Dev Biol 76:58–78.

Weisblat DA, Kim SY, Stent GS. 1984. Embryonic origins of cells in the leech Helobdella triserialis. Dev Biol 104:65–85.

Whitman CO. 1878. The embryology of Clepsine. Q J Microsc Sci 18:213–315.

Wilson EB. 1892. A cell-lineage of Nereis: a contribution to the cytogeny of the annelid body. J Morphol 6:361–481.

Zackson SL. 1982. Cell clones and segmentation in leech development. Cell 31:761–770.

Zackson SL. 1984. Cell lineage, cell-cell interaction, and segment formation in the ectoderm of a glossiphoniid leech embryo. Dev Biol 104:143–160.

Zhang SO, Weisblat DA. 2005. Applications of mRNA injections for analyzing cell lineage and asymmetric cell divisions during segmentation in the leech Helobdella robusta. Development 132: 2103–2113.